2005 International Symposium on Nonlinear
Theory and its Applications (NOLTA2005)
Bruges, Belgium, October 18-21, 2005

Measurement and Numeric Calculation for Printed Spiral Inductors

Mizuki Motoyoshi†, Yoshiei Tanaka‡, Masayuki Ymauchi‡ and Mamoru Tanaka‡

†Department of Electronics Engineering, School of Engineering, The University of Tokyo,
7-3-1, Hongou, Bunkyo-ku, Tokyo 113-8656, Japan
‡Department of Electrical and Electronics Engineering, Sophia University,
7-1, Kioi-cho, Chiyoda-ku, Tokyo 102-8554, Japan
Email: motoyoshi@m.ieice.org, yoshiei@tlab.ee.sophia.ac.jp

Abstract—**In this paper, circular spiral inductor is composed on a printed board. Specifications of the spiral inductor is closely investigeted by actual measurements and numerical calculations. Further, PS-Inductors are designed by using our proposed numerical calculation method. Our proposed method is verified availability on applications which include some PS-Inductors.**

1. Introduction

Recently, a flat inductor as a spiral is used as a chip inductor, on-chip inductor and so on[1][2]. The flat inductor called "spiral inductor." Further, an inductor of same style and large scale is used as an antenna and is called "spiral antenna." These elements are very important and often used. However, in many systems, a mutual inductance is not used as mutual inductance, because influences of a magnetic field to other elements are problems and it is necessary to use a core of magnetic material. In many systems with a mutual inducance, a transformer with an iron core is used. The transformer with an iron core is very heavy and large.

In this research, a spiral inductor that is composed on a printed wiring board is called "Printed Spiral Inductor (PS-Inductor)." Specifications of the PS-Inductors are closely investigated by using experiments and numerical calculations. Further, a FM-Demodulator is made by using mutual inductance between multilayer PS-Inductors, which are designed by our numerical calculation method. Our design method is verified availability on applications.

2. Printed Spiral Inductor

In this research, PS-Inductor is created by combining semicircular patterns. A single-sided substrate is used in measurement of a inductance, and a double-sided substrate is used for verification of our method.

2.1. Measurements

In a PS-Inductor created by combining semicircle, the layout and inductance are decided by five parameters shown in Fig.1. Each parameter is fixed to each value in Fig.1, and inductance is measured while changing number of half-turns.

2.1.1. Method of Measurement

The inductance is measured by oscillating system which is built by combining arbitrary capacitors to a PS-Inductor. When the LC-Oscillation is caused,

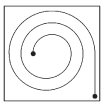

Greatest diameter : $Fmax = 36[mm]$
Pattern distance : $d = 0.2[mm]$
Pattern width : $w = 0.1[mm]$
Pattern thickness : $35[\mu m]$ (single-sided), $9[\mu m]$ (double-sided)
Number of half-turn : $t = 40, 60, 60, 100, 110$ *and* $115[half\text{-}turn]$
Board material : Glass epoxy

Figure 1: Printed Spiral Inductor.

inductance is obtained from the oscillation frequency and the capacitances. The oscillation frequency is changed by changing values of capacitors. And, a mean value of the obtained inductances is adopted as value of true inductance.

Measuring of inductance of high accuracy involves oscillation frequency and capacitance of high accuracy. Therefore, when inductance is measured, parasitic impedance must be removed by all possible means in the experiment circuit and the calculation. The colpitts oscillation circuit which uses only one bipolar-transistor is used for to reduce influence of parasitic impedance. The circuit is shown in Fig.2. Synthetic capacitance (C_0) and oscillation frequency (f_0) in this circuit are represented by following equations respectively (see Eq.(1)).

$$f_0 = \frac{1}{2\pi\sqrt{LC_0}}\ ,\ C_0 = C_4 + \frac{1}{\dfrac{1}{C_1}+\dfrac{1}{C_2}+\dfrac{1}{C_3}} \qquad (1)$$

In this experiment, frequency measurement and wavy observation are done with a digital oscilloscope because influences of various equipment must be removed to a maximum extent. When the inductance is obtained, values of parasitic capacitance of transistor, parasitic capacitance of oscilloscope and parasitic impedance of probe must be included into calculation. Actual measurement values before considering parasitic impedances are shown in Fig.3(a). An equivalent circuit of measuring impedance is shown in the frame of Fig.2. The inductance with mesuring impeadance is shown as Eq.(3). And, measurement results considering parasitic impedances are shown in Fig.3(b).

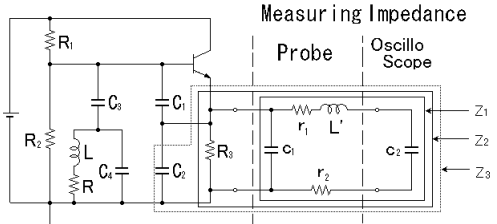

Figure 2: Collpits Oscillator and Equivalent Circuit of Measuring Device.

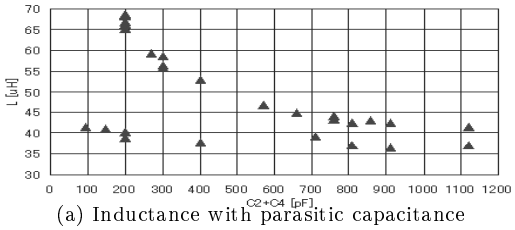

(a) Inductance with parasitic capacitance

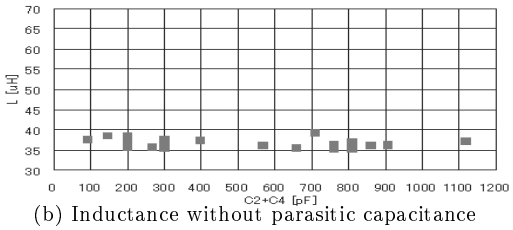

(b) Inductance without parasitic capacitance

Figure 3: Estimation of Inductance(Inductance vs. Capacitance).

$$\left.\begin{aligned} Z_1 &= \frac{1}{\mathrm{j}\omega c_1 + \dfrac{1}{r_1 + \mathrm{j}\omega L' + r_2 + \dfrac{1}{\mathrm{j}\omega c_2}}} \\ Z_2 &= \frac{1}{\dfrac{1}{R_3} + \dfrac{1}{Z_1}} \\ Z_3 &= \frac{1}{\dfrac{1}{Z_2} + \mathrm{j}\omega C_2} = \frac{\gamma + \mathrm{j}\omega\delta}{\alpha + \mathrm{j}\omega\beta} \end{aligned}\right\} \quad (2)$$

where

$$\begin{aligned} \alpha &= 1 - \omega^2(r_1 + r_2)R_3c_2(c_1 + C_2) - \omega^2 c_2 L' \\ \beta &= R_3(c_1 + c_2 + C_2) + c_2(r_1 + r_2) \\ &\quad -\omega^2 L' R_3 c_2(c_1 + C_2) \\ \gamma &= R_3 - \omega^2 c_2 R_3 L' \ , \quad \delta = (r_1 + r_2)c_2 R_3 \\ \varepsilon &= \frac{\alpha R_3 + \omega^2\beta\gamma}{\alpha^2 + \omega^2\beta^2} \\ \zeta &= -\frac{1}{\omega}\left(\frac{1}{C_1} + \frac{1}{C_3}\right) + \frac{\omega(\alpha\gamma - \beta R_3)}{\alpha^2 + \omega^2\beta^2} \end{aligned}$$

$Z_1 \sim Z_3$ are shown in Fig.2 respectively.
AC-Analysis is applied to the circuite and the circuit equation is solved.

The inductance(L) is obtained by using oscillation condition from circuite equation. That is under the condition of circuit equation's imaginary part equal zero.

$$L = \frac{1 + \sqrt{1 - 4\eta^2 R^2}}{2\omega\eta} \quad (3)$$

where

$$\eta = (\omega C_4 + \frac{-\zeta}{\varepsilon + \zeta})$$

2.1.2. Results

The measurement result of inductance is shown in Fig.7 and Q-factor is shown in Fig.8. The PS-Indutor has extremum of value. In these parameters of PS-Inductor, maximum inductance is observed around 100[*turns*]. Q value is roughly hundreds of levels and is very high.

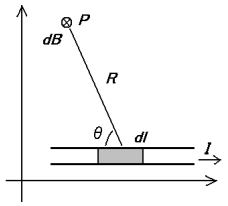

Figure 4: Biot-Savart

2.2. Numerical calculation of inductance

In this research, diameter of PS-Inductor changes at each semicircle. So, an inductance is obtained not by using generic theoretical analysis but by using the Biot-Savart Law and the finite element method. Calculation uses same parameters as actual measurement. Further, calculation uses values of the parameters as actual measurement. However the thickness of the conductor is not considered.
In Fig.4, magnetic flux density (dB) at an arbitrary point(P) which is created by current (Idl) on imperceptible interval of direct-current electricity (I) is obtained by Biot-Savart Law. When Biot-Savart Law is applied and integrated along the conductor, magnetic flux density at point P which is made by entire current is obtained. In this research, analysis area is divided into sectors, and the finite element method is used for the sectors respectively. Esach sector of analysis target and reference point have four parameters as follows: (see Fig.5)

1. Maximum angle of central angle (φ_{cmin} and φ_{tmin}).
2. Minimum angle of central angle (φ_{cmax} and φ_{tmax}).
3. Maximum radius (r_{cmin} and r_{tmin}).
4. Minimum radius (r_{cmax} and r_{tmax}).

Because interlinkage magnetic flux decreases as a more outside area is analyzed, the accuracy of analysis does not fall, though area of analysis incleases as a more outside area is analyzed. Further, the problem is solved by using an analytical angle very small. In addition, the current distribution is assumed as a same value in the whole area of the conductor. Considering about distributed constant is needed in the high frequency band, but considering about distributed constant is not needed in this research, because analysis target circuits are up to about some few mega hertz.

2.2.1. Setting of coordinate

In this paper, each abbreviation of reference point and analysis point of Biot-Savart Law and finite element method is set as follows:

AT : A sector of analysis target of magnetic flux between conductors.
AT_c: Coordinate of analysis point in AT.
SC : Sectoral conductor of reference area of analysis.

SC_c: Coordinate of analysis reference point in SC.
AT_c and SC_c are set as follows:

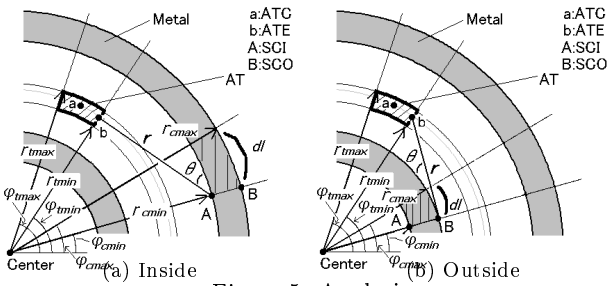

(a) Inside (b) Outside

Figure 5: Analysis.

1. **SC_c:** Two coordinates are set to edge of inside and outside of SC respectively (see "A" and "B" in Fig.5). The inside coordinate (SCI_c) is set as follows:

$$(SCI_{c_x}, SCI_{c_y}) = (r_{cmin}\cos(\varphi_{cmin}), r_{cmin}\sin(\varphi_{cmin})) \quad (4)$$

The outside coordinate (SCO_c) is set as follows:

$$(SCO_{c_x}, SCO_{c_y}) = (r_{cmax}cos(\varphi_{cmin}), r_{cmax}sin(\varphi_{cmin})) \quad (5)$$

If AT exists from tangent at SCI_c on the center point side, SCI_c is used as coordinate of reference point. If AT exists in an area between tangent of SCI_C and tangent of SCO_C the AT is not calculated from the SC. And, otherwise, SCO_C is used.

2. **AT_c:** Two coordinates of AT_c are set (see "a" and "b" in Fig.5). A coordinate of center point of an arc which splits square measure of AT to two area is set as ATC_c (see "a" in Fig.5).

$$(ATC_{c_x}, ATC_{c_y}) = (r\cos(\varphi), r\sin(\varphi)) \quad (6)$$

where

$$r = \sqrt{\frac{r_{tmin}^2 + r_{tmax}^2}{2}}$$

$$\varphi = \frac{\varphi_{tmin} + \varphi_{tmax}}{2}$$

A coordinate of φ_{tmin} of an arc which splits square measure of AT to two area is set as ATE_c (see "b" in Fig.5).

$$(ATE_{c_x}, ATE_{c_y}) = (r\cos(\varphi_{tmin}), r\sin(\varphi_{tmin})) \quad (7)$$

where

$$r = \sqrt{\frac{r_{tmin}^2 + r_{tmax}^2}{2}}$$

A magnetic flux density which is generated from SC becomes maximum value when a distance between AT_c and SC_c becomes to minimum value. Further, the magnetic flux density becomes to maximum value when $sin\theta = 1$ (see Eq.(9)). Therefore, as an analytical angle is reduced, a result of using ATC_c becomes big (see Fig.6-a), and a result of using ATE_c becomes small (see Fig.6-b). In this research, an analytical angle is fixed 1[degree]. The mean value of inductance by using ATC_c and inductance by using ATE_c is assumed a true value.

Value of dl in SC is needed to apply Biot-Savart Law. Because SC has width, dl is not constant in a SC. An arc of outside of SC is longer than an arc of inside of SC. In this research, because computational effort is decreased, dl is assumed to length of arc which

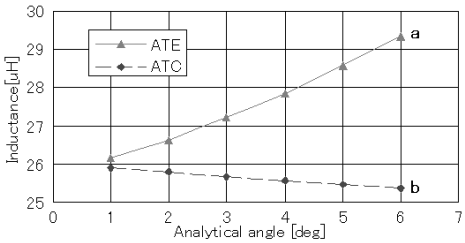

Figure 6: Calculation result by difference of analytical coordinates position.

splits square measure of AT to two area.

$$dl = \sqrt{\frac{r_{cwin}^2 + r_{cmax}^2}{2}} \times \frac{\theta_a}{360} \quad (8)$$

where

$\theta_a = (\varphi_{tmax} - \varphi_{tmin}) = (\varphi_{cmax} - \varphi_{cmin})$ $[degree]$

Inside of the conductor does not be analyzed.

2.2.2. Calucation of magnetic flux density

Firstly, magnetic flux densities are calculated at each AT. A magnetic flux density in a AT which is generated by one SC at time t is calculated by Biot-Savart Law. Total magnetic flux density in a AT is calculated by applying to all SC (see Eq.(9)).

$$B_n(t) = \sum_{m=1}^{M} \frac{\mu_0}{4\pi} \frac{i(t) \cdot \sin(\theta(n,m)) \cdot dl(m)}{\{r(n,m)\}^2} \quad (9)$$

where

$n : AT\ number\ ,\quad m : SC\ number$

2.2.3. Calculation of inductance

Inductance is obtained by equation Eq.(10).

$$L = \frac{d\Phi(t)}{di(t)} \quad (10)$$

Φ shows the interlinkage magnetic flux in PS-Inductor.

Therefore, when inductance of one semicircle is obtained, interlinkage magnetic flux in the semicircle must be obtained. It is named Φ_{N_I} that total interlinkage magnetic of inside of the semicircle. The expression from which semicircle inductance L is requested becomes Eq.(12). Inductance (L) of the semicircle is shown as follows:

$$\begin{cases} B_m(t) = \sum_{p=1}^{N_C} A(m,p) \cdot i(t) \\ \Phi_{N_I}(t) = \sum_{m=1}^{N_I} B_m(t) S_m \end{cases} \quad (11)$$

$$L = \frac{\Delta\Phi_{N_I}(t)}{\Delta i(t)} = \sum_{m=1}^{N_I} \left(\sum_{p=1}^{N_C} A(m,p) \right) \cdot S_m \quad (12)$$

where

$$A(m,p) = \frac{\mu_0}{4\pi} \frac{\sin(\theta(m,p)) \cdot dl(p)}{\{r(m,p)\}^2}$$

$N_I : total\ sectoral\ number\ of\ inside\ target\ from\ a\ half\ circle$

$N_C : total\ sectoral\ number\ of\ conductor\ on\ a\ half\ circle$

$m : AT\ number$

$p : SC\ number$

The inductance of each semicircle is replaced as L_k ($1 < k < N_C$). PS-Inductor can be expressed by connecting

all semicircle inductors in series. Therefore, PS-Inductor (L_{Total}) can be expressed as follows:

$$L_{Total} = \sum_{k=1}^{N_{HC}} L_k \qquad (13)$$

where

$$N_{HC} : \textit{Numbe of half circles}$$

Each parameter is set as follows:

1. Analysis minimum angles : 1 [degree]
2. Number of partitions in the vertical direction between conductors : 10

The calculation result is shown in Fig.7.

In Fig.7, the numerical calculation result well accords with the actual measurement value. And, an extremum is observed in the numerical calculation result as well as the actual measurement value. Difference between the actual measurement value and the numerical calculation value is observed in vicinity of extremal value. The difference is assumed influence of a wire for measurement because the wire for measurement exists in area of high magnetic flux density.

Next, Fig.8 shows the result of Q-Factor. The numerical calculation result well accords with the actual measurement value, too.

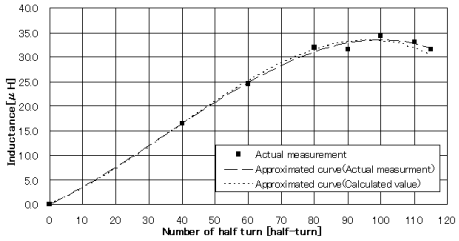

Figure 7: Inductance of PS-Inductor.

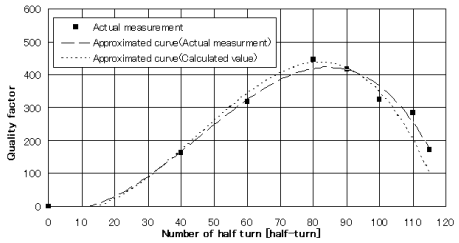

Figure 8: Quality factor of PS-Inductor.

3. Verification of our design method

We design a PS-Inductor by using our numerical calculation method. By a FM-Demodulator with the PS-Inductors is made, our design method is verified availability on applications. PS-Inductor is composed like the plane, so mutual inductance can be easily used by using the multilayer substrate. In this study, FM Demodulator by slope detection is made by a double sided substrate of 5[cm] corner as shown in Fig.9. But, one diode and one capacitor are used as an external element respectively. The tuning circuit designed a center frequency as 5.0[MHz]. Because 1000[pF] had been used as capacitance, inductance was designed as 1.0[uH].

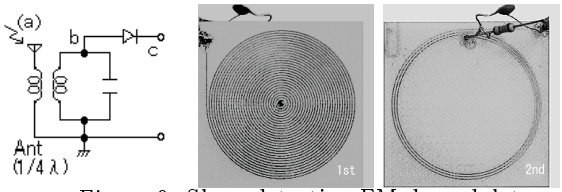

Figure 9: Slope detection FM demodulator.

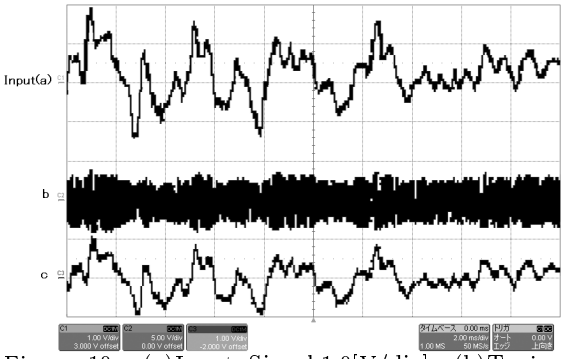

Figure 10: (a)Input Signal:1.0[V/div], (b)Tuning Output:5.0[V/div], (c)Detection Output:1.0[V/div].

A tuning curve is shown in Fig.11, and a result of demodulation is shown in Fig.10. Figure 10(a) is shown a signal before modulating. Figure 10(b) is shown an output signal of tuning. Figure 10(c) is shown an output signal of detection. Because signals (a) and (c) are similar shapes, it is understood that the FM signal is perfectly demodulated by using the mutual inductance. Therefore we consider the designed PS-Inductor showed the characteristic the same as the design value, and operation of the circuit according to the expectation.

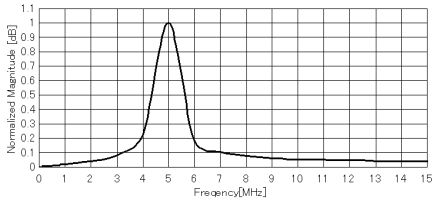

Figure 11: Tuning curve.

4. Conclusion

In this study, PS-Inductors was obtained by using experiments and numerical calculations. Actual measurement values and the numerical calculation results were overlapping very well. Thus, inductances can be obtained by this measuring method and calculation method.

It was understood that an extremum exists in the inductance and Q-Factor from the result. The number of turns at extremum of Q-Factor differed from the number of turns at extremum of inductance.

We designed a PS-Inductor by using our numerical calculation method. By a FM-Demodulator with the PS-Inductors is made, our design method was verified availability on applications. The center frequency of the tuning curve, which is measurement result, corresponded with the design value. Therefore, our proposal method is able to design a inductor in high accuracy.

Acknowledgment

This research is supported by the fund of Open Research Center Project from MEXT of Japanese Government (2002-2006).

References

[1] Kenichi OKADA, "Design Optimization Methodology for On-Chip Spiral Inductors," IEICE Trans. Electron., Vol.E87-C, no.6, June, 2004.

[2] H.G. Dill, "Designing Inductors for Thin Film Applications," Electronic Design, pp.52-59, 1964.

[3] Sunderarajan S. Mohan, "Simple Accurate Expressions for Planar Spiral Inductances," IEEE Jounal of solid-state circuits., Vol.37, no.10, Oct, 1999.